# A SURVEY OF RECENT DEVELOPMENTS IN THE EVALUATION OF STRESS INTENSITY FACTORS FROM ISOCHROMATIC CRACK-TIP FRINGE PATTERNS

H.P. Rossmanith* and R. Chona**

*Inst. f. Mechanics, Technical University, Vienna, Austria
**Dept. of Mechanical Engineering, University of Maryland, College Park, MD., USA

## ABSTRACT

This paper surveys and discusses recent developments in general aspects of analysis related to the determination of opening-mode stress intensity factors from isochromatic fringe data. Various methods are applied to selected fringe patterns from different fracture test specimens, and considerable emphasis is placed on comparing the values of K obtained from the different evaluation procedures used.

## KEYWORDS

Linear elastic fracture; isochromatic fringe patterns; stress intensity factors; Westergaard-type stress functions; higher order terms.

## INTRODUCTION

The study of the stress and strain fields around the base of stationary and running cracks is fundamental to fracture mechanics. Under linear-elastic conditions, both stresses and strains display a singular behaviour at the crack tip, with the stress intensity factor, K, providing a convenient measure of the magnitude of the singularity. A single parameter characterization of the crack tip stress field in terms of K is generally recognized as adequate for engineering practice and is valid if attention is restricted to a very small region around the crack tip (the singularity-dominated zone).

Frequently however, crack tip stress field regions that are too large for a one-parameter representation become of interest, either due to a growth in size of the fracture process zone or as a practical consequence of experimental methods for the determination of K. For example, even in a brittle solid, roughening of the fracture due to spreading out of advance cracking (secondary flaw opening) and incipient branching substantially enlarge the fracture process zone. As a second example, isochromatic fringes in the immediate vicinity of the crack tip may be visibly distorted (Fig. 1a) or the crack tip region may be obscured by a pseudo-caustic formed due to light-scattering at the crack tip (Fig. 1b). In addition, for reasons such as crack front curvature, fringe clarity, an unknown degree of plane strain constraint close to the crack tip, etc., data taken from fringes further away from the crack tip would be less prone to error and hence preferable.

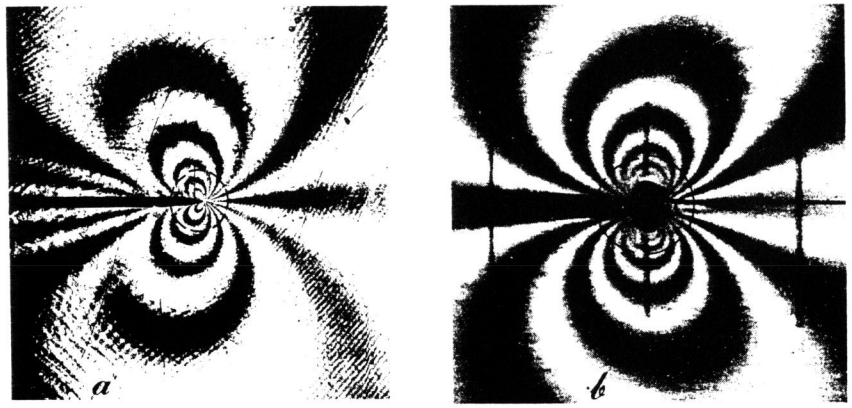


Fig. 1 Experimentally obtained isochromatic fringe patterns illustrating (a) the visible distortion of fringes close to the crack tip and (b) masking of the crack tip region by a caustic-type formation.

A general analytical basis for stress field representations will be presented in this paper and the historical development of K-determination methods will be summarized. For brevity, examples of experimentally obtained static isochromatic fringe patterns around opening-mode cracks in three representative standard fracture test specimens will be analyzed using several different methods and the results compared.

## THE DEVELOPMENT OF K-DETERMINATION PROCEDURES

During the 1950's, Post (1955) drew attention to the advantageous use of photoelastic techniques for the study of crack-tip stress fields. A subsequent photoelastic investigation of propagating cracks was made by Wells and Post (1958) using the technique of high-speed photography. Irwin (1958a), in a discussion to that paper, suggested a simple engineering approach for the determination of K-values from the isochromatic patterns of a mode-1 crack. Irwin's analysis was based on the Westergaard-type stress function approach (Westergaard, 1939; Irwin, 1958b), and represents a special case of Muskhelishvili's method. To better match the experimentally recorded fringe patterns with analytically generated ones, Irwin introduced an additional uniform stress field, $\sigma_{ox}$, which acts parallel to the crack line, and in an infinite specimen, does not contribute to the stress intensity factor. This additional stress field, which cannot be directly incorporated in the classical Westergaard function, Z(z), represents a far-field influence on the stress pattern, and is proportional to the $\alpha$-term, or more precisely, the $A_o$-term in the analysis that is given in a subsequent part of this paper.

Irwin's method made use of the fact that for a given fringe ($\tau_m$=constant), $\partial\tau_m/\partial\theta$ is zero at the apogee point of an isochromatic fringe such as that shown in Fig. 2. A measurement of the apogee distance, $r_m$, and the fringe loop tilt, $\theta_m$, can then be used to obtain the value of K and $\alpha$, using $K_n$, an expression for the normalized stress intensity factor, based upon a two-parameter (static or dynamic) solution (Etheridge and Dally, 1977; Rossmanith and Irwin, 1979; Dally, 1979), where

$$\tau_m = \frac{K}{\sqrt{2\pi r}} F_2(r, \theta, c, \alpha^*) \qquad (1)$$



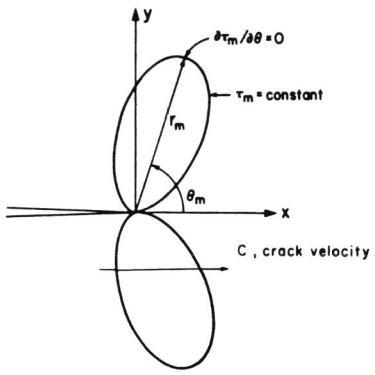


Fig. 2 Geometry and coordinates for a typical pair of isochromatic fringe loops.

and

$$K_n \equiv \frac{K}{2\tau_m\sqrt{2\pi r_m}} = H_2(r_m, \theta_m, c, \alpha^*) \qquad (2)$$

with $\alpha^* \equiv \sigma_{ox}\sqrt{2\pi r}/K$ and c = crack speed.

It is generally recognized that eqn (1) adequately describes the state of stress in the immediate neighbourhood of the crack tip, excluding a very small region around the crack tip itself. The region of validity of this equation is however quite restricted and the problem is complicated by the transition in the local neighbourhood of the crack tip, from a state of plane strain to generalized plane stress. This occurs even in thin specimens, and the size of this transition region for purely elastic specimens is of the order of one-half the plate thickness. To avoid this region of uncertainty, and for some of the reasons mentioned previously and illustrated in Fig. 1, the experimental stress analyst is constrained to take measurements in regions which may lie outside the range of validity of the two-parameter stress field representation. It thus becomes necessary to use parameters additional to K and $\alpha$ to provide an adequate representation of the stress field in an enlarged region around the crack tip and to better match experimentally recorded and analytically generated fringe patterns (Etheridge, 1976). Considerable work in this area has taken place in the past decade.

Particular attention has been paid by Rossmanith and Irwin (1979) and Rossmanith (1979, 1980) to the effects of including a first higher order term proportional to $z^{\frac{1}{2}}$, which is the lowest order non-singular term in the Westergaard-type stress function, Z(z). This term is referred to as the $\beta$-term or the $B_1$-term in the subsequent discussion. Using a three-parameter representation in terms of K, $\alpha$, and $\beta$, the shape of an isochromatic fringe loop becomes

$$\tau_m = \frac{K}{\sqrt{2\pi r}} F_3(r, \theta, c, \alpha^*, \beta^*) \qquad (3)$$

with the normalized stress intensity factor, $K_n$, given by

$$K_n \equiv \frac{K}{2\tau_m\sqrt{2\pi r_m}} = H_3(r_m, \theta_m, c, \alpha^*, \beta^*) \qquad (4)$$

The evaluation of the desired parameters can be accomplished in a number of different ways. A logical extension of an analysis based on one or two fringe is to take advantage of the full field data available from isochromatic fringes, and develop a method of K-determination based on a finite set of measurement points. These points might lie on different fringe loops (and hence may belong to different levels and states of stress) and could be either randomly distributed (Klein, 1974; Sanford and Dally, 1979; Irwin and co-workers, 1979) or selected in some particular fashion (Rossmanith and Irwin, 1979; Chona, Irwin and Shukla, 1980). The use of a non-linear least squares technique can be easily combined with an overdetermined set of simultaneous equations from a large number of data points (Klein, 1974; Sanford and Dally, 1979; Irwin and co-workers, 1979; Sanford, 1980), and can be

conveniently used for analyses based on an n-parameter approach to the problem.

In general, the shape of an isochromatic fringe loop for a mode-1 propagating crack can be represented by

$$\tau_m = \left| \text{Re } X_a + i \text{ Im } X_b \right| \tag{5}$$

where the complex functions $X_a$ and $X_b$ are linear combinations of suitably chosen Westergaard-type functions, $Z_1$, $Z_2$, $Y_1$, and $Y_2$ (Irwin, 1980). For static cracks, eqn (5) reduces to (Sanford, 1979; Rossmanith, 1981)

$$\tau_m = 2 \left| Y + \tfrac{1}{2} i \, (z - \bar{z})(Z' + Y') \right| \tag{6}$$

where the stress functions are suitably chosen to be

$$Z(z) = \sum_{n=0}^{N} B_n z^{n-\frac{1}{2}} \quad \text{and} \quad Y(z) = \sum_{m=0}^{M} A_m z^m \tag{7}$$

from which, $K = B_o\sqrt{2\pi}$; $\alpha^* = \alpha\sqrt{r/r_s} = 2\sqrt{r/r_s}\, A_o/B_o$; and $\beta^* = \beta r/r_s = r_s\, B_1/B_o$. Here, $r_s$ is a scaling length, which may be assigned a value typical of the size of the measurement region being used. The upper limits N and M in eqn (7) denote the number of half-integer and integer power terms being retained in the analysis. A summary of K-determination methods and their associated index pairs (N,M) is given in Table I. As an example, a six-parameter method (N=M=2) calls for the simultaneous evaluation of K or $B_o$, $A_o$, $B_1$, $A_1$, $B_2$, and $A_2$.

TABLE I Summary Showing the Historical Development of K-Determination Procedures

| Number of Parameters Retained in the Analysis | Number of Data Points Used: 1 | 2 | large |
|---|---|---|---|
| 1 | | | Static (0,-) C.W. Smith, 1972 |
| 2 | Static (0,0) Irwin, 1958<br>Dynamic (0,0) Irwin et al, 1975 | Static (0,0) Bradley and A.S. Kobayashi, 1970 | Static (0,0) Sanford and Dally, 1979<br>Dynamic (0,0) Irwin et al, 1979 |
| 3 | Static and Dynamic (1,0) Dally and Etheridge, 1978; Rossmanith and Irwin, 1979 | Static and Dynamic (1,0) Rossmanith and Irwin, 1979 | Static and Dynamic (1,0) University of Maryland, Photomechanics Lab., 1979-1980 |
| Arbitrary | | | Static and Dynamic (N,M) University of Maryland, Photomechanics Lab., 1979-1980 |



## ILLUSTRATIVE EXAMPLES AND DISCUSSION

Figure 3 shows the geometries of the three standard fracture test specimens used as examples in this paper. In each case, the figure shows the crack tip location in the specimen, as well as the region around the crack tip used for data acquisition purposes. The fringe patterns obtained experimentally are shown in Figs. 4a, 5a, and 6a, for the SEN, MCT, and RDCB specimens respectively.

Each fringe pattern was analyzed to obtain the values of the associated parameters using several different methods of K-determination. The methods used ranged from

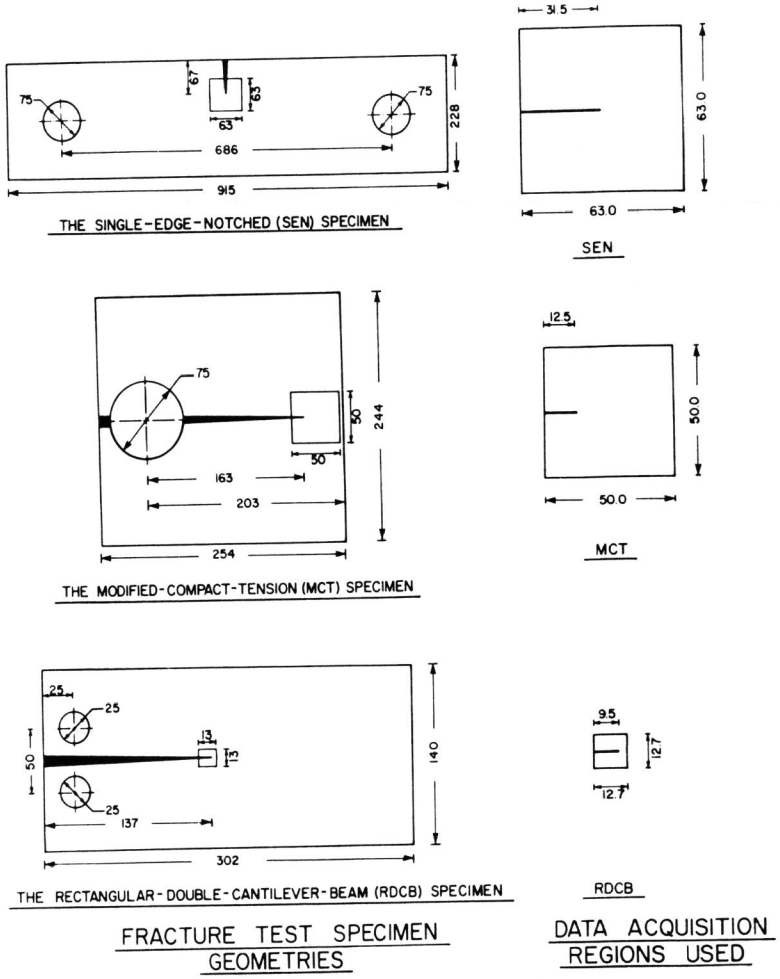


Fig. 3 Geometry and dimensions of the standard fracture test specimens used showing the relative location of the crack in the specimen.

a 2-parameter apogee point technique to a 6-parameter least squares solution. The fringe patterns corresponding to the parameter values obtained by different methods have been plotted and are shown in Figs. 4b-4d for the SEN specimen, Figs. 5b-5d for the MCT specimen, and Figs. 6b-6d for the RDCB specimen. All plots have been drawn to the same scale as the experimental photograph for easier comparison.

In the case of the SEN specimen, the main loops ($N \geq 2.5$) are predicted quite well by all the four solutions shown. However, differences in the shape and location of the 0.5 and 1.5 order fringes are readily apparent. The computed value of K varies a small amount from the apogee point (N=3.5) to the 3-parameter solution (1.68 to 1.74 MPa-$m^{\frac{1}{2}}$), but the computed value of $\alpha$ is appreciably different when a 3-parameter solution is used, changing from -0.42 to -0.33, or almost 50%. This

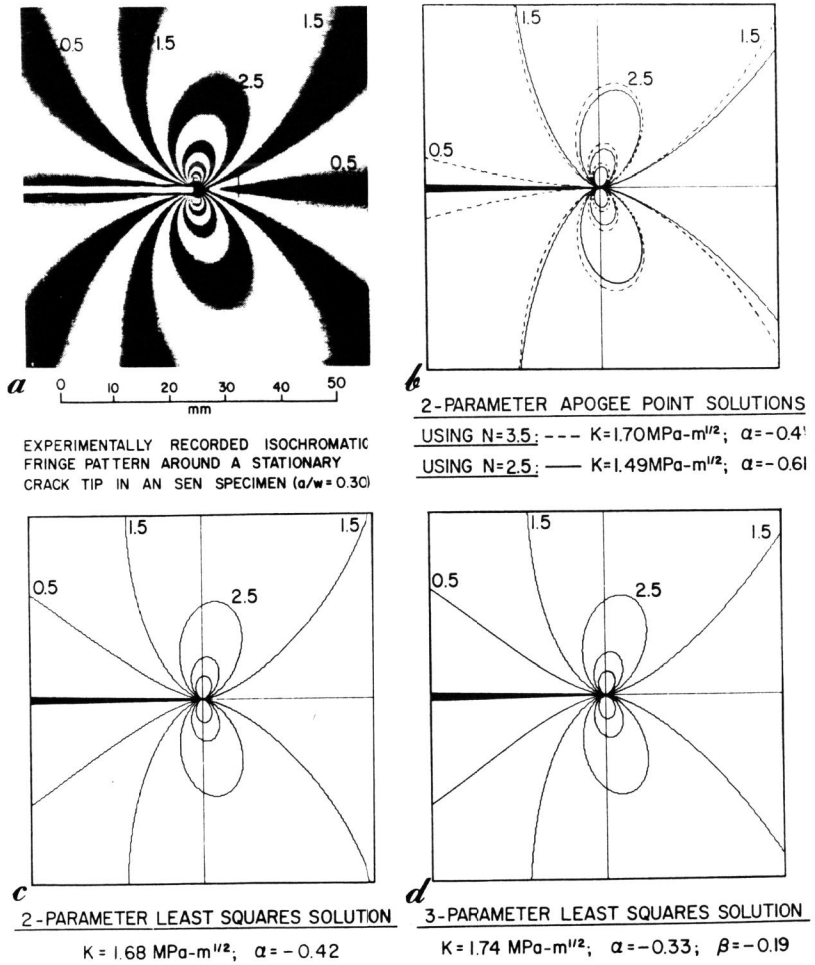


Fig. 4 Experimentally recorded isochromatic fringe pattern from an SEN specimen and the predicted fringe pattern and parameter values corresponding to the different K-determination methods used.



is quite consistent with previously reported results (Chona, Irwin and Shukla, 1980) and is to expected since fringe loop tilt and shape are both affected by $\alpha$ and $\beta$.

The MCT example shown in Fig. 5 represents a rather deep crack (a/w=0.80), and the fringe pattern of Fig. 5a has obvious boundary influences present. The 2-parameter apogee point and least squares solutions completely fail to predict the salient features of the actual fringe pattern. The 3-parameter least squares solution, although capable of matching medium-sized main loops (N=3.5 to N=5.5) quite well, does not correctly predict the fringe distribution ahead of the crack tip. The fringes produced by the steep gradient field ahead of the crack require the use of at least a 6-parameter solution (M=N=2, Fig. 5d) before the global appearance of

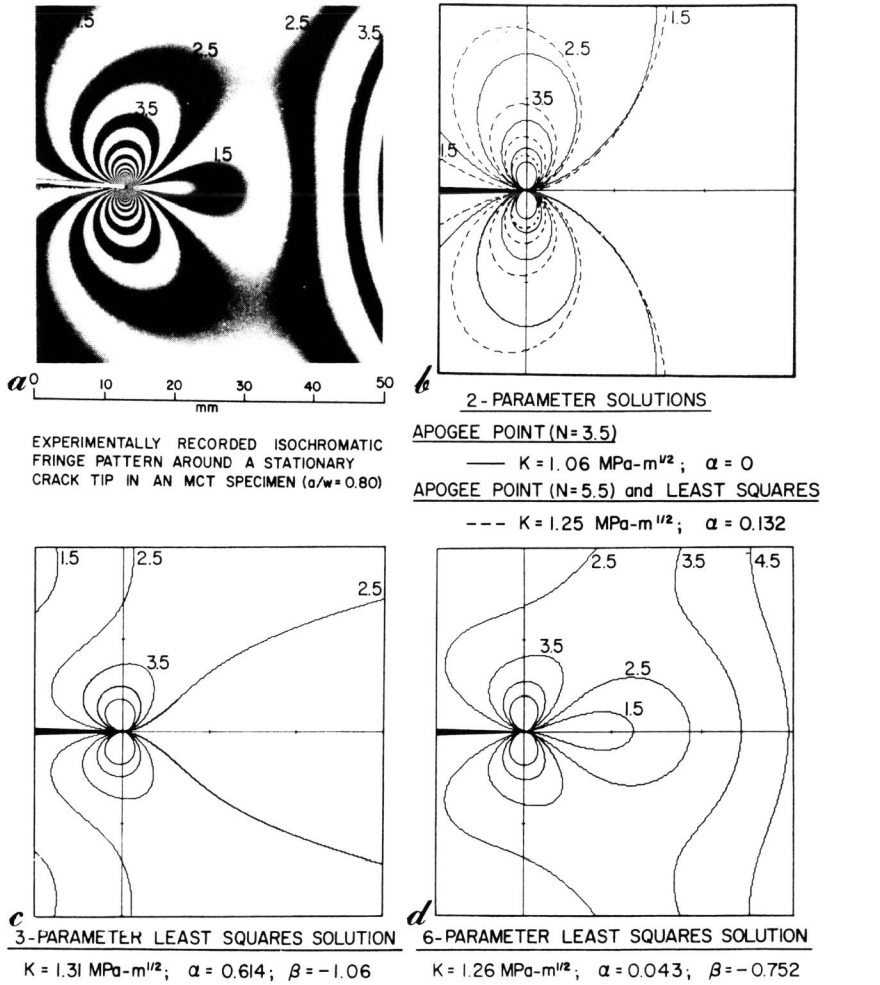


Fig. 5 Experimentally recorded isochromatic fringe pattern from an MCT specimen and the predicted fringe pattern and parameter values corresponding to the different K-determination methods used.

the predicted fringe pattern begins to match that seen experimentally. However, differences still exist between Figs. 5a and 5d, indicating that for the crack location and data acquisition region used, a model of order higher than six may well be required. Notice, that the variations in K are similar to those of the SEN specimen example, with computed values ranging from 1.25 to 1.31 MPa-$m^{\frac{1}{2}}$ using 2-parameter through 6-parameter least squares solutions. Once again, variations in computed values of $\alpha$ are larger (0.043 to 0.614) and changes in $\beta$ are also quite significant (-0.732 to -1.06).

In the RDCB example shown in Fig. 6, fringes of order $N \geq 3.5$ are matched fairly well by both 2-parameter and 3-parameter solutions. However, the shape and

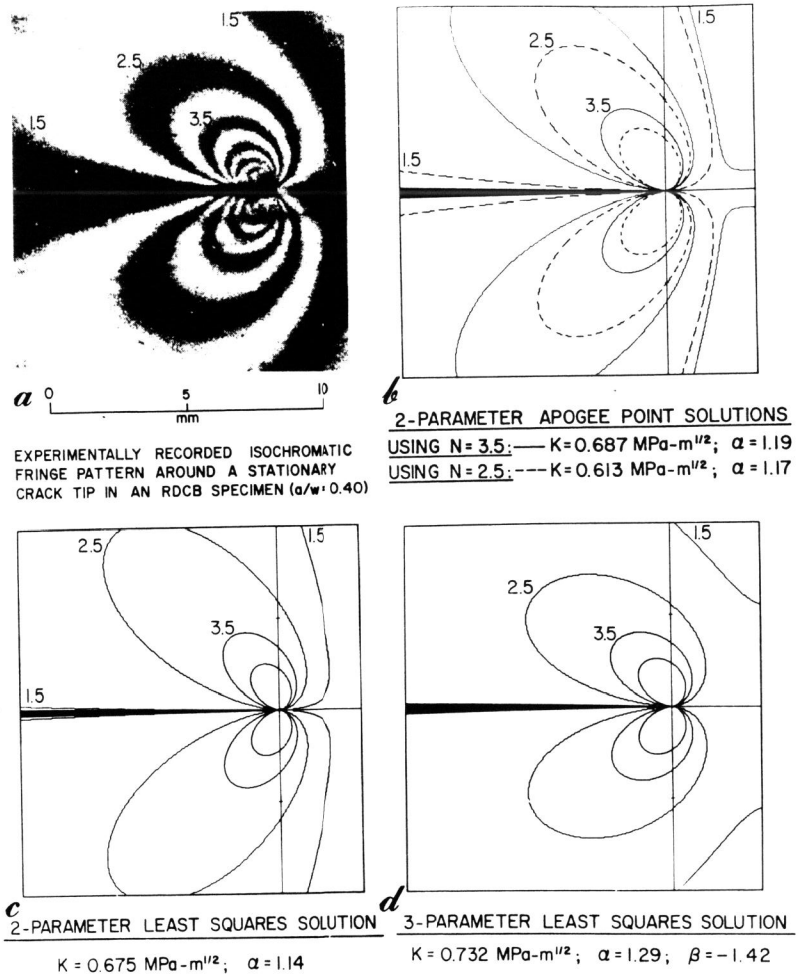


Fig. 6 Experimentally recorded isochromatic fringe pattern from an RDCB specimen and the predicted fringe pattern and parameter values corresponding to the different K-determination methods used.



orientation of fringes of order 2.5 or less are only adequately modelled after the introduction of the $\beta$-term. The specimen used was 9.5 mm thick, and even the fringe of order 2.5 lies quite close to the crack tip. Variations in K-values as determined from the different methods are small (0.675 to 0.732 MPa-$m^{\frac{1}{2}}$) but the $\alpha$-term changes more, and especially after the $\beta$-term is introduced, since it is quite large.

## CONCLUSIONS

In summation, it can be seen from the examples presented, that adequate modelling of the stress state present can require the retention of as many as six terms in eqn (7) and that reliable values of both K and $\alpha$ can only be obtained when the solution includes at least the $B_0$, $A_0$, and $B_1$ terms. Rossmanith and Irwin (1979) have provided a summary in tabulated form of the characteristic features of the fringe patterns observed in different standard specimens, and this is reproduced here as Table II, to provide a guide for the reader who is actually involved in K-determination using isochromatic fringe patterns. It is worth mentioning that the least squares method, by utilising data from a global field is preferable to a single-point, apogee-type method, and is likely to give more reliable results. It is also the only method available which permits the simultaneous determination of more than three parameters.

The increase in complexity of the analysis for a constant speed running crack (Irwin, 1980) is moderate. For the case of a non-uniformly propagating crack, the invariance of the higher order terms has not been established to date. Some preliminary results on the variation of higher order terms with crack extension may be found in Rossmanith and Irwin (1979) and Chona, Irwin and Shukla (1980). Further work in this area is currently in progress.

TABLE II Characteristic Features of Fringe Patterns in Standard Test Specimens*

| Loop Tilt | Loop Shape | $\alpha$ and $\beta$ Values | K-field | Specimen Type |
|---|---|---|---|---|
| Highly Forward | Slim | $\alpha < 0, \beta < 0$ | Increasing | SEN |
| Forward | Moderate | $\alpha < 0, \beta \simeq 0$ | | SEN |
| Forward | Standard | $\alpha \simeq 0, \beta < 0$ | | SEN |
| Straight Up | Broad | $\alpha < 0, \beta < 0$ | Gradually Decreasing | MCT |
| Straight Up | Standard | $\alpha \simeq 0, \beta \simeq 0$ | | MCT |
| Slightly Backward | Moderate | $\alpha \simeq 0, \beta > 0$ | | MCT |
| Backward | Slim | $\alpha > 0, \beta > 0$ | Decreasing | RDCB |
| Backward | Standard | $\alpha > 0, \beta \simeq 0$ | | RDCB |
| Highly Backward | Broad | $\alpha >> 0, \beta < 0$ | | RDCB |

* - Adapted from Rossmanith and Irwin (1979).
Note: The influence of increasing crack speed is primarily to increase the tilt.

## ACKNOWLEDGEMENTS

This research work has been sponsored in part by the Fonds zur Forderung der wissenschaftlichen Forschung in Austria under Contract No. 3864 to H.P. Rossmanith and in part by the Nuclear Regulatory Commission through Subcontract No. 7778 (Oak Ridge National Laboratory) to the University of Maryland Photomechanics Laboratory. Support for the computer time required was provided by the UOM Computer Science Ctr.

REFERENCES

Chona, R., G.R. Irwin, and A. Shukla (1980). A comparison of two and three parameter representations of the stress field around static and dynamic cracks. *Experimental Mechanics*. (To appear).

Dally, J.W. (1979). Dynamic photoelastic studies of fracture. *Experimental Mechanics, 19*, 349-367.

Etheridge, J.M. (1976). *Determination of the Stress Intensity Factor K from Isochromatic Fringe Loops*. University of Maryland Ph.D. Dissertation, College Park, MD., USA.

Etheridge, J.M., and J.W. Dally (1977). A critical review of methods for determining stress-intensity factors from isochromatic fringes. *Experimental Mechanics, 17*, 248-254.

Irwin, G.R. (1958a). Discussion of: The dynamic stress distribution surrounding a running crack -- A photoelastic analysis. *Proc. SESA, XVI*, 93-96.

Irwin, G.R. (1958b). Fracture. In *Handbuch der Physik, Vol. VI*, Springer, Berlin. pp. 558-590.

Irwin, G.R. (1980). Fracture analysis using photoelastic data. In *Lecture Series on Fracture Mechanics, Part IV*, Institute for Physical Science and Technology, University of Maryland, College Park, MD., USA.

Irwin, G.R., W.L. Fourney, D.B. Barker, J.T. Metcalf, R.J. Sanford, A. Shukla, and R. Chona (1979). *Photoelastic Studies of Damping, Crack Propagation, and Crack Arrest in Polymers and 4340 Steel*. U.S. NRC Report NUREG/CR-1455, Washington, D.C., USA.

Klein, G. (1974). *A Method for the Determination of Mixed-Mode Stress Intensity Factors and its Application to a Crack in the Neighbourhood of a Circular Hole* (in German). Inst. f. Werkstoffmechanik Report, Freiburg, West Germany.

Post, D. (1955). Photoelastic stress analysis for an edge crack in a tensile field. *Proc. SESA, XII*, 99-116.

Rossmanith, H.P. (1979). Fringe-loop dynamics and crack branching. In *Proceedings of the IUTAM Symposium on Optical Methods in Mechanics of Solids*, Poitiers, France, September 10-14, 1979.

Rossmanith, H.P. (1980). A dynamic three-parameter method for determination of stress intensity factors from isochromatic crack-tip fringe patterns. *J. Appl. Mech.* (To appear).

Rossmanith, H.P. (1981). The method of caustics for static plane elasticity problems. *J. of Elasticity*. (To appear).

Rossmanith, H.P., and G.R. Irwin (1979). *Analysis of Dynamic Isochromatic Crack-Tip Stress Patterns*. Department of Mechanical Engineering Report, University of Maryland, College Park, MD., USA.

Sanford, R.J. (1979). A critical re-examination of the Westergaard method for solving opening-mode crack problems. *Mech. Res. Comm., 6*, 289-294.

Sanford, R.J. (1980). Application of the least-squares method to photoelastic analysis. *Experimental Mechanics, 20*, 192-197.

Sanford, R.J., and J.W. Dally (1979). A general method for determining mixed-mode stress intensity factors from isochromatic fringe patterns. *Engr. Fract. Mech., 11*, 621-633.

Wells, A., and D. Post (1958). The dynamic stress distribution surrounding a running crack -- A photoelastic analysis. *Proc. SESA, XVI*, 69-92.

Westergaard, H.M. (1939). Bearing pressures and cracks. *Trans. ASME, 61*, A49-A53.